In Silico Computation of Electrograms and Local Electrical Impedance to Assess Non-Transmural Fibrosis

Carmen Martínez Antón[1], Jorge Sánchez[2], Nansi Caslli[1], Lena Heinemann[1], Laura Anna Unger[1,3], Axel Loewe[1], Olaf Dössel[1]

[1] Institute of Biomedical Engineering, Karlsruhe Institute of Technology (KIT), Karlsruhe, Germany
[2] ITACA Institute, Universitat Politècnica de València, Valencia, Spain
[3] Medizinische Klinik IV, Städtisches Klinikum Karlsruhe, Karlsruhe, Germany

Abstract

Regions with pathologically altered substrate have been identified as potential proarrhythmic regions for atrial fibrillation. Mapping techniques, such as voltage mapping, are currently used to estimate the location of these fibrotic areas. Recently, local impedance (LI) has gained attention as another modality for atrial substrate assessment as it does not rely on the dynamically changing electrical activity of the heart. However, its limits for assessing non-transmural and complex fibrosis patterns have not yet been characterized in detail. In this work, we study the ability of EGMs and LI to identify non-transmural fibrosis in different transmural locations using in silico experiments. Models were developed to simulate both the voltage and the LI maps. A pseudo-bidomain model was used to recover the extracellular potential on the surface of the tissue while LI reconstruction was calculated by a time-difference imaging approach with an homogeneous tissue background conductivity. Four different fibrosis configurations were modeled to compare the two modalities (voltage map and LI map) using the Pearson correlation coefficient. Only one transmural structure was detected by voltage whereas all non-transmural structures, namely endocardial, midmyocardial, and epicardial, yielded zero value. The correlation for LI maps ranged from -0.02 to 0.74. We conclude that LI can be used in combination with EGMs to account for fibrotic substrate. LI values are expected to distinguish between healthy atrial tissue and fibrotic areas, which paves the way towards the use of LI as a surrogate for non-transmural atrial fibrosis substrate.

1. Introduction

Atrial fibrillation (AF) is the most common cardiac arrhythmia and it is associated with a remodeling of the atrial substrate. A standard treatment for AF is ablation, which involves creating lesions in the pulmonary veins to isolate them. In patients with persistent AF, additional ablation lesions can be placed in areas of fibrotic tissue, which can include complex fibrotic patterns that fractionate the wavefront and could potentially promote reentries [1].

During an ablation procedure, mapping techniques are currently used to estimate the location of these abnormal substrate areas. Electrograms (EGMs) can be recorded in a unipolar or bipolar technique [2] and can be used to produce local activation time (LAT) and voltage maps to represent the electrical activity of the heart.

While EGM-based substrate mapping has shown inconclusive success, recently, local impedance (LI) has been gaining attention as a surrogate to differentiate pathologically altered substrate due to its independence on the electrical activity [3]. LI may improve the current understanding of underlying substrate, including the possibility of computing full-chamber maps [4].

In this work, we study the ability of EGMs and LI to identify non-transmural fibrosis areas in different locations of the endo-, midmyo-, and epicardium using in silico experiments. By using an intracardiac electrical impedance tomography (EIT) system applied to a multielectrode mapping catheter [5], we aim to explore the possibility to differentiate fibrotic tissue located on the midmyo- and epicardial surface where EGMs lose track of the atrial substrate.

2. Methods

An in silico squared patch of tissue measuring 36 mm $\times$ 36 mm $\times$ 2.5 mm was embedded in a 40 mm $\times$ 40 mm $\times$ 25 mm box that represents the surrounding blood (Figure 1). A circular catheter with 10 zero-dimensional point electrodes in a spatial arrangement mimicking the Lasso™ catheter (Biosense Webster, Irvine, CA, USA) with a radius of 7.5 mm, was placed centrally above the tissue.

Centered below the catheter, 4 fibrosis patterns with different levels of entropy [6] as shown in Figure 2 were

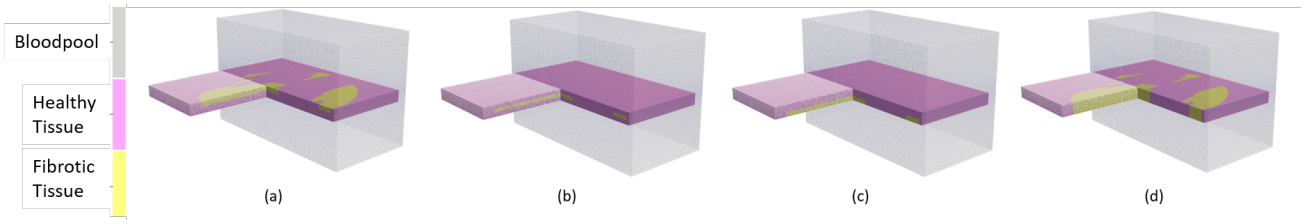

Figure 1. Geometrical model setup of one exemplary fibrosis patch in its distinct configurations with cuts along two planes for visualization purposes. Each tissue is surrounded by a blood bath (grey) and its cells are assigned as healthy (pink) or fibrotic (yellow). (a) Endocardial: fibrosis area on the surface of the tissue patch. (b) Midmyocardial: fibrosis area in the middle of the tissue patch. (c) Epicardial: fibrosis area at the bottom of the tissue patch. (d) Transmural: fibrosis area throughout the total thickness of the tissue patch.

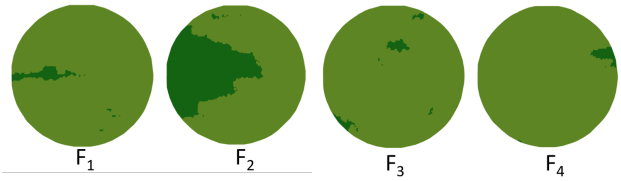

Figure 2. Ground truth of each fibrosis pattern: F_{1-4}. Light green represents healthy tissue, whereas dark green areas are assigned to fibrosis. F_2 and F_4 show the lowest and highest entropy, respectively.

placed. Each pattern was realized with 4 distinct configurations: endo-, midmyo-, epicardial, and transmural. For the endo-, midmyo-, and epicardial cases, the thickness of the fibrotic area was set to 1.25 mm, i.e., half of the total tissue thickness, varying only its location along the z-axis. The transmural configuration occupied the totality of the tissue thickness. In total, 16 different configurations were studied. Meshes comprising 1,020,544 tetrahedral elements were generated using Gmsh [7].

2.1. Electrogram computation

Electrical propagation in the tissue and its surroundings was simulated by solving the pseudo-bidomain model in openCARP [8]. Cellular electrophysiology was modeled using the ionic model proposed by Courtemanche et al. [9]. A stimulus was placed at one lateral face of the tissue to simulate a planar wavefront.

For healthy tissue, 0.36 S/m and 1.29 S/m, were set as intracellular and extracellular conductivity, respectively [10]. The fibrotic region was modeled with a conductivity of 10^{-5} S/m, and 0.7 S/m was assumed for the blood [11].

The extracellular potentials of each point within 9 mm radius measured from the center of the catheter at the surface of the tissue were extracted to compute voltage maps. At each point, the peak-to-peak (p2p) voltage was computed as the difference between the maximum and the minimum value over time. As suggested in [12], a bipolar voltage threshold of 1 mV corresponds to a unipolar threshold of 1.32 mV.

2.2. Local electrical impedance simulation

The local electrical impedance simulation was performed as described in [5]. The spread of the electrical field was modeled using the software EIDORS [13] in MATLAB (The MathWorks, Inc., Natick, MA, USA, version 2021a). An alternating current of 5 mA peak-to-peak amplitude at 14.5 kHz was simulated. Conductivity values at body temperature for blood, healthy tissue, and connective tissue at f = 14.5 kHz were modeled as 0.7 S/m, 0.164 S/m, and 0.387 S/m , respectively [14].

Stimulation, i.e. current injection, was performed from adjacent electrode pairs. For each set of simulations, each bipolar pair was chosen to be the stimulating pair once and measuring bipole the rest of the times, sticking to four-terminal circuits during all sets. Laplace discrete regularization with $\lambda = 10^{-7}$ was applied. A time-difference imaging approach with a homogeneous tissue background conductivity σ_{BI} = 0.164 S/m was employed.

On a two-dimensional mesh, three dimensional electrode positions were projected to the surface to perform an inverse reconstruction. The enclosed surface was extended radially by 1.5 mm and meshed with triangles of an average edge length of 0.2 mm.

2.3. Comparison between the modalities

To compare both mapping techniques, the Pearson correlation coefficient between the two binarized images and the ground truth of each fibrosis configuration was computed.

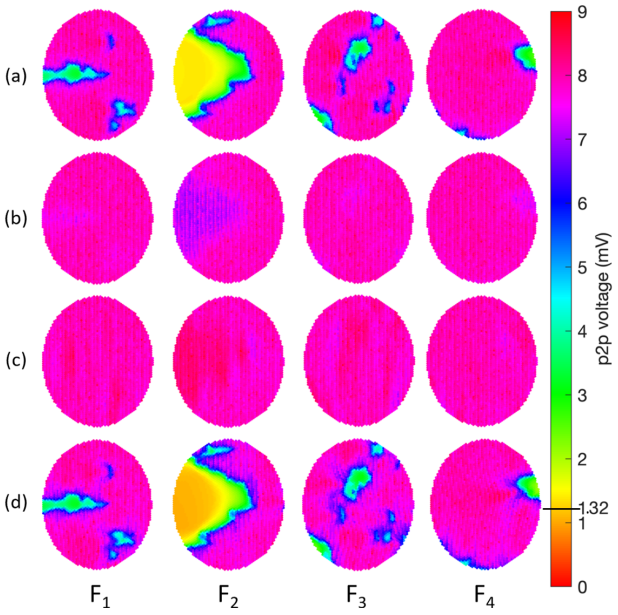

Figure 3. Continuous voltage maps of each setting: endocardial (a), midmyocardial (b), epicardial (c), and transmural (d), of four different fibrosis configurations F_{1-4}. Low voltage threshold at 1.32 mV is depicted.

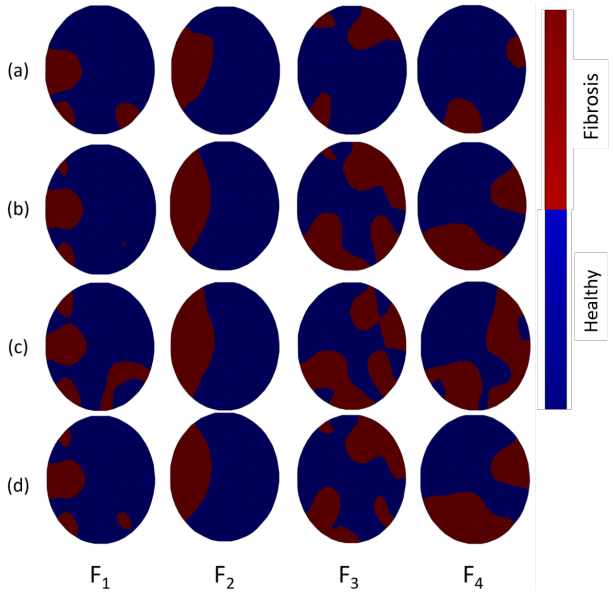

Figure 4. Binary reconstructed structures of each setting: endocardial (a), midmyocardial (b), epicardial (c), and transmural (d), of four different fibrosis configurations F_{1-4}.

3. Results

3.1. Voltage maps

As shown in Figure 3, no fibrosis was recognized for any midmyo- or epicardial structure. Fibrotic structures not located on the surface yielded high voltage values, whereas endocardial and transmural configurations were better identified. However, after applying the voltage threshold, only F_2 in the transmural configuration led to some low voltage extent with a correlation of 0.7.

3.2. LI maps

Differences in conductivity compared to the respective background image were reconstructed. For all the configurations and patterns, fibrotic structures were identified (Figure 4). Reconstruction quality varied by pattern, increasing as the entropy of the pattern decreased (Table 1).

In the transmural case, the correlation values ranged between 0.16 and 0.72, whereas values between 0.25 and 0.74 were obtained for the endocardial configuration. For midmyo- and epicardial configurations, lower absolute value correlations between 0.03 and 0.68 were observed.

Among the different patterns, correlation values of 0.68, 0.68, 0.72, and 0.74 were obtained for F_2 in midmyocardial epicardial, transmural and endocardial configurations, respectively. For the smaller patterns $F_{1,3,4}$, mean correlation values decreased respectively to 0.29, 0.18, and 0.17. A negative correlation of -0.02 was found for F_3 in midmyocardial configuration.

Table 1. Correlation values between ground truth structures and relative conductivity reconstruction (LI maps) for each pattern F_{1-4} (columns) and configuration (rows).

	F_1	F_2	F_3	F_4	Mean
Endocardial	0.29	0.74	0.25	0.32	0.40
Midmyocardial	0.24	0.68	0.10	-0.02	0.27
Epicardial	0.33	0.68	0.15	0.18	0.34
Transmural	0.32	0.72	0.19	0.16	0.35
Mean	0.29	0.70	0.17	0.17	

4. Discussion

In a previous study [5], simple fibrosis patterns were used to explore the capabilities of this new *in silico* method to account for conductivity changes. Up to the authors' knowledge, no previous works evaluated the ability of voltage and LI maps to account for realistic fibrosis patterns while examining non-transmural fibrosis configurations in tissue.

Voltage maps were not able to detect any diffuse fibrosis pattern except for F_2 in the transmural configuration, which presents the lowest entropy. The threshold used to identify low voltage regions might be too low for this *in silico* setting and could be optimized in future work. LI

maps yielded slightly better fibrosis detection. Endocardial configurations showed the best results on average, whereas midmyocardial ones performed worst. Among the fibrotic patterns, F_2 led to an average correlation value of 0.70 due to its compactness. For the voltage maps, both configuration and thickness of the fibrotic area were proven to be of importance. On the other hand, LI can detect fibrosis located at different locations in a similar extent but the size of the structure is clearly of importance. However, reconstructed conductivity values were thresholded according to the distance to each relative maximum value. The threshold is a balance between over- and undersensing of potential arrhythmogenic substrate.

In this study, only a circular catheter setting was employed. The lack of electrodes outside of the circumferential shape leads to a loss of information when the structures are located at the innermost parts of this area. Using other catheter setups, such as the Advisor™ HD Grid (Abbott, Chicago, IL, USA) or the Sphere-9™ (Medtronic, Dublin, Ireland) could improve the reconstruction quality when accounting for smaller fibrotic patches located centrally.

In summary, this *in silico* comparison helped to better understand the limits of using voltage for fibrosis detection, as it may lead to underestimation of non-transmural areas. LI can detect fibrotic areas which are big enough, which can improve the understanding of underlying substrate and paves the way towards the use of impedance as a readout for non-transmural atrial fibrosis substrate.

5. Conclusions

An *in silico* evaluation of voltage and LI-based mapping techniques as a surrogate for atrial substrate was conducted. In locations in which voltage maps were not able to detect any fibrosis extent, the LI reconstruction led to higher correlation values in critical fibrotic areas. More catheter and fibrosis configurations with more complex electrical propagation simulations should be implemented for further analysis in the future.

Acknowledgments

This work was supported by the European Union's Horizon 2020 research and innovation programme under the Marie Skłodowska-Curie grant agreement No 860974 (PersonalizeAF), and by the European High-Performance Computing Joint Undertaking EuroHPC under grant agreement No 955495 (MICROCARD).

References

[1] Jellis C, Martin J, Narula J, Marwick TH. Assessment of nonischemic myocardial fibrosis. Journal of the American College of Cardiology 2010;56(2):89–97.

[2] Kusumoto FM. Understanding Intracardiac EGMs and ECGs. John Wiley & Sons, 2011.

[3] Martin CA, Martin R, Gajendragadkar PR, Maury P, Takigawa M, Cheniti G, Frontera A, Kitamura T, Duchateau J, Vlachos K, Bourier F, Lam A, Lord S, Murray S, Shephard E, Pambrun T, Denis A, Derval N, Hocini M, Haissaguerre M, Jais P, Sacher F. First clinical use of novel ablation catheter incorporating local impedance data. Journal of Cardiovascular Electrophysiology 2018;29(9):1197–1206.

[4] Unger LA, Schicketanz L, Oesterlein T, Stritt M, Haas A, Martínez Antón C, Schmidt K, Dössel O, Luik A. Local electrical impedance mapping of the atria: Conclusions on substrate properties and confounding factors. Frontiers in Physiology 2022;12.

[5] Unger LA. Multimodal Characterization of the Atrial Substrate - Risks and Rewards of Electrogram and Impedance Mapping. Ph.D. thesis, 9 2022.

[6] Sánchez J, Trenor B, Saiz J, Dössel O, Loewe A. Fibrotic remodeling during persistent atrial fibrillation: In silico investigation of the role of calcium for human atrial myofibroblast electrophysiology. Cells ;10(11).

[7] Geuzaine C, Remacle JF. Gmsh: A three-dimensional finite element mesh generator with built-in pre- and post-processing facilities. International Journal for Numerical Methods in Engineering 2009;79.

[8] Plank G, Loewe A, Neic A, Augustin C, Huang YL, Gsell MA, Karabelas E, Nothstein M, Prassl AJ, Sánchez J, et al. The opencarp simulation environment for cardiac electrophysiology. Computer methods and Programs in Biomedicine ;208.

[9] Courtemanche M, Ramirez RJ, Nattel S. Ionic mechanisms underlying human atrial action potential properties: insights from a mathematical model. American Journal of Physiology Heart and Circulatory Physiology ;275(1).

[10] Nairn D, Hunyar D, Sánchez Arciniegas J, Doessel O, Loewe A. Impact of electrode size on electrogram voltage in healthy and diseased tissue. 12 2020; .

[11] Abdalla S. Low frequency dielectric properties of human blood. IEEE Transactions on NanoBioscience 2011;10(2).

[12] Nairn D, Lehrmann H, Müller-Edenborn B, Schuler S, Arentz T, Dössel O, Jadidi A, Loewe A. Comparison of unipolar and bipolar voltage mapping for localization of left atrial arrhythmogenic substrate in patients with atrial fibrillation. Frontiers in Physiology ;11.

[13] Adler A, Lionheart WRB. Uses and abuses of EIDORS: an extensible software base for EIT. Physiological Measurement 2006;27.

[14] Gabriel C. Compilation of the Dielectric Properties of Body Tissues at RF and Microwave Frequencies. Texas, USA: Occupational and Environmental Health Directorate, Radiofrequency Radiation Division, Brooks Air Force Base, 1996. Report N.AL/OE-TR-1996-0037.

Address for correspondence:

Carmen Martínez Antón, publications@ibt.kit.edu
Institute of Biomedical Engineering, Karlsruhe Institute of Technology (KIT), Kaiserstr. 12, 76131, Karlsruhe, Germany